Journal of Neonatal Surgery
ISSN(Online): 2226-0439
Vol. 14, Issue 32s (2025)
https://www.jneonatalsurg.com

OPEN ACCESS

Development and In-Vitro Characterization of Transdermal Delivery Carrier Niosomal Gel of Low Oral Bioavailability Drug Pravastatin Sodium

Nikhil[1], Ankit Kumar[1], Kuldeep kumar[2], Anjana devi[3*]

[1]Research scholar, Department of Pharmacy, Career Point University, Hamirpur, (H.P)-176041

[2]Associate Professor, Department of Chemistry, Career Point University, Hamirpur (H.P)-176041

[3]Associate Professor, Department of Pharmacy, Career Point University, Hamirpur (H.P)-176041

[*]**Corresponding author:**

Anjana devi

Associate Professor, Department of Pharmacy, Career Point University, Hamirpur (H.P)-176041

Email ID: anjana.pharmacy@cpuh.edu.in

Cite this paper as: Nikhil, Ankit Kumar, Kuldeep kumar, Anjana devi, (2025) Development and In-Vitro Characterization of Transdermal Delivery Carrier Niosomal Gel of Low Oral Bioavailability Drug Pravastatin Sodium. *Journal of Neonatal Surgery*, 14 (32s), 2650-2665.

ABSTRACT

Pravastatin sodium, a widely prescribed HMG-CoA reductase inhibitor, suffers from poor oral bioavailability due to extensive first-pass metabolism and limited intestinal permeability. To overcome these limitations, the present study focuses on the development and in-vitro characterization of a transdermal delivery system in the form of a niosomal gel. Niosomes, non-ionic surfactant-based vesicles, were prepared using the thin-film hydration technique with varying ratios of Span 60 and cholesterol. The optimized niosomal formulations were incorporated into a Carbopol 934 gel base to obtain the final niosomal gel formulations. These formulations were evaluated for physicochemical parameters such as pH, viscosity, spread ability, homogeneity, and drug content, which were found to be within acceptable ranges for topical application. In-vitro drug release studies using Franz diffusion cells demonstrated a sustained release profile over 24 hours. The optimized formulation, G2DPN14, showed the highest cumulative drug release (96.95%), followed by G3DPN14 (81.17%), significantly outperforming the control gel. The release kinetics of G2DPN14 followed Higuchi's model, indicating a diffusion-controlled mechanism. The enhanced release and stability of the drug within the gel matrix suggest effective encapsulation and prolonged drug delivery potential. Overall, the study confirms that pravastatin sodium-loaded niosomal gel is a promising approach for transdermal drug delivery, offering advantages such as bypassing first-pass metabolism, prolonged release, and improved patient compliance. Future in-vivo and clinical studies are warranted to establish its therapeutic efficacy and safety for the management of hyperlipidaemia and associated cardiovascular conditions.

Keywords: *Pravastatin sodium, Niosomes, Transdermal delivery, Niosomal gel, In-vitro characterization, Bioavailability enhancement*

1. INTRODUCTION

Pravastatin sodium is a hydrophilic statin widely used for the treatment of hypercholesterolemia and the prevention of cardiovascular diseases. It acts as a competitive inhibitor of the enzyme 3-hydroxy-3-methyl-glutaryl-coenzyme A (HMG-CoA) reductase, the rate-limiting step in cholesterol biosynthesis. By blocking this enzyme, pravastatin effectively reduces low-density lipoprotein (LDL) cholesterol and triglycerides while modestly increasing high-density lipoprotein (HDL) cholesterol levels(Neuvonen, Niemi, and Backman 2006). Despite its efficacy, the oral bioavailability of pravastatin sodium is significantly low (~18%) due to its poor intestinal permeability and extensive first-pass hepatic metabolism (Hatanaka 2000). Conventional oral delivery of pravastatin presents pharmacokinetic limitations, including erratic absorption, degradation in the gastrointestinal tract, and hepatic first-pass metabolism, which necessitates frequent dosing and increase the risk of systemic side effects (Reinoso, Telfer, and Rowland 1997). These challenges underscore the need for alternative delivery systems that can bypass hepatic metabolism and provide sustained drug release. Transdermal drug delivery offers a promising alternative to the oral route by facilitating controlled drug release through the skin directly into systemic circulation, thereby bypassing first-pass metabolism. Transdermal systems not only improve patient compliance due to ease of application but also reduce dose frequency and maintain steady-state plasma concentrations (Prausnitz and Langer 2008).

However, the stratum corneum, the outermost layer of the skin, presents a significant barrier to drug permeation, especially for hydrophilic drugs like pravastatin sodium(Marais 2019). To enhance skin permeation, nanoscale vesicular systems such as Niosomes have been widely explored. Niosomes are non-ionic surfactant-based vesicles that encapsulate both hydrophilic and lipophilic drugs, improving drug stability, permeability, and controlled release properties(Manosroi et al. 2012). They offer several advantages including low toxicity, biodegradability, ease of production, and higher entrapment efficiency compared to traditional carriers. Furthermore, the incorporation of niosomes into a gel base enhances the topical application by improving viscosity, spread ability, and residence time at the application site(Furumoto et al. 2004). Hence, the present study aims to develop and characterize a niosomal gel formulation of pravastatin sodium for transdermal delivery to enhance its bioavailability and therapeutic efficacy. The formulation was evaluated for particle size, entrapment efficiency, morphology, in-vitro drug release, and permeation characteristics. As demonstrated in Figure 1.1, topical niosomal gel treatment enhances drug retention in the skin's outermost layers, passing through the stratum corneum (SC) to the viable layers of the epidermis (VE) and, to a lesser degree, the dermis' upper layer.

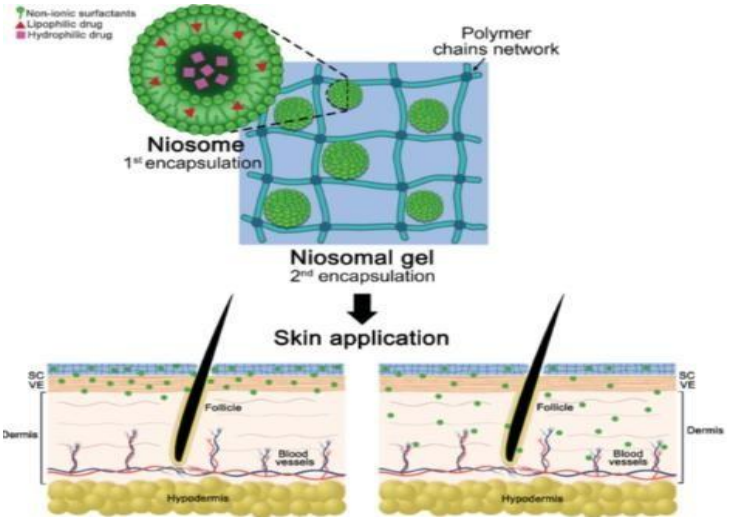

Figure 1.1. Schematic representation of niosomal gel for encapsulation of lipophilic and hydrophilic drugs for skin application.

2. MATERIALS AND METHODS

2.1 Materials

Pravastatin sodium was obtained as a gift sample from Cipla Ltd., Baddi, Himachal Pradesh, India. India. Non-ionic surfactants Span 60 and Tween 60 were purchased from Sisco Research Laboratories (SRL), Mumbai, India. Cholesterol was obtained from HiMedia Laboratories Pvt. Ltd., India. Carbopol 934 and hydroxypropyl methylcellulose (HPMC K4M) were procured from Loba Chemie, Mumbai. All other chemicals and solvents used were of analytical grade and used as received without further purification. Double-distilled water was used throughout the study.

2.2 Preparation of Niosomes

Niosomes were prepared using the thin-film hydration method. Briefly, accurately weighed quantities of Span 60, cholesterol, and pravastatin sodium were dissolved in a mixture of chloroform and methanol (2:1, v/v) in a round-bottom flask. The solvent mixture was evaporated under reduced pressure using a rotary evaporator at 60 ± 2°C to form a thin lipid film on the flask wall. The film was then hydrated with phosphate-buffered saline (PBS, pH 7.4) by rotating the flask at room temperature for 1 hour. The resulting niosomal suspension was sonicated to reduce particle size and achieve a uniform dispersion.

2.3 Formulation of Niosomal Gel

The niosomal suspension was incorporated into a gel base prepared using Carbopol 934. Carbopol 934 was soaked in distilled water overnight and neutralized with triethanolamine to achieve a pH suitable for skin application (5.5–6.5). Propylene glycol was added as a humectant. The niosomal dispersion was then mixed uniformly with the gel base to obtain the final niosomal gel.

Table no 1 Composition of the pravastatin sodium loaded niosome containing different surfactant

S.No.	Formulation code	Amount of drug (mg)	Amount of surfactant (Molar)				
			Span 60	Span 80	Tween 80	Tween 60	Amount of cholesterol (Molar)
1	PN1	68	7	-	-	-	3
2	PN2	68	-	7	-	-	3
3	PN3	68	-	-	7	-	3
4	PN4	68	-	-	-	7	3

2.4 Evaluation of Niosomal Gel

The prepared gels were evaluated for the following parameters:

pH: Measured using a digital pH meter.

Viscosity: Determined using a Brookfield viscometer.

Spreadability: Evaluated by parallel plate method.

Homogeneity: Assessed by visual inspection.

Drug Content: Quantified by UV-visible spectrophotometry at λmax 239 nm after suitable dilution with phosphate buffer.

In-vitro Drug Release: Performed using Franz diffusion cells with cellophane membrane and phosphate buffer pH 7.4 as receptor medium. Samples were withdrawn at predetermined intervals and analyzed spectrophotometrically.

Release Kinetics: Drug release data were fitted to various kinetic models (zero-order, first-order, Higuchi, and Korsmeyer-Peppas) to determine the mechanism of drug release.

Formulation of Niosomal Gel: The optimized niosomal dispersion was incorporated into a Carbopol 934 gel base, neutralized with triethanolamine, and evaluated for pH, viscosity, spread ability, and drug content.

Optimization Parameters: The formulation was optimized by varying the Span 60: cholesterol molar ratio (e.g., 1:1, 2:1, 3:1), hydration volume (10–20 mL), and surfactant type (Span vs. Tween) to achieve maximum entrapment efficiency and desired particle size

Evaluation Parameters:

Particle size and zeta potential: Measured using dynamic light scattering.

Entrapment efficiency (EE%): Determined by centrifugation and spectrophotometric analysis.

In-vitro release: Performed using Franz diffusion cells with cellophane membrane.

In-vitro permeation: Carried out using rat abdominal skin.

3. RESULTS AND DISCUSSION

3.1 Preformulation Studies

- **Organoleptic Properties**

The melting point was recorded as 140.0°C ±1.00 to 141.34°C ±1.53, in agreement with reported literature values (140–

142°C), confirming the drug's identity and purity (148)

- **UV Absorption Maxima**

The absorption maxima (λmax) of pravastatin sodium in methanol was found to be 239 nm using UV spectrophotometry, closely matching the literature value of 238 nm (148) (Figure 1).

Figure 1: UV spectrum of pravastatin sodium (10 µg/ml in methanol)

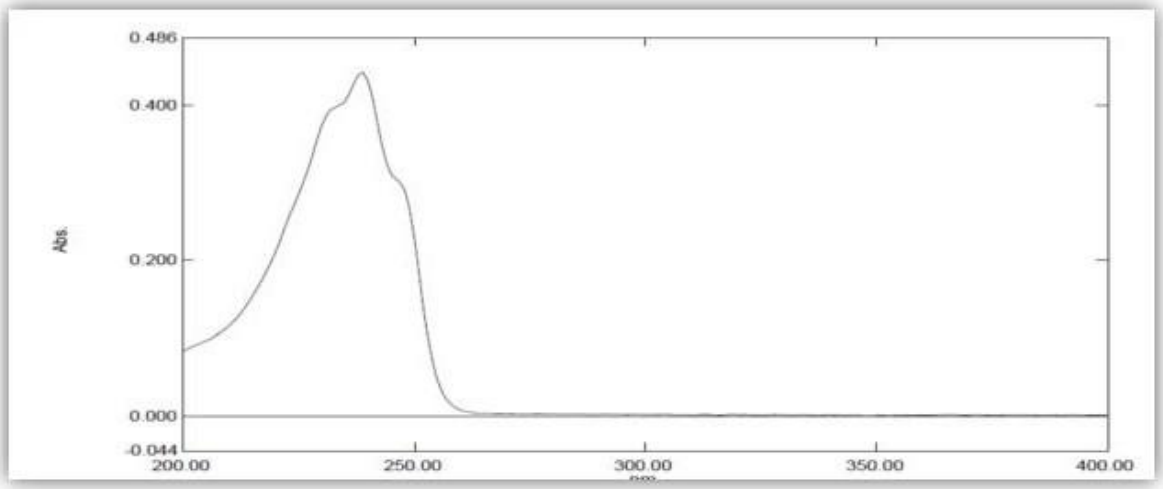

- **Standard Calibration Curve**

A calibration curve in the range of 2–20 µg/ml showed excellent linearity (R^2 = 0.999) with the regression equation Y = 0.0458x + 0.0085 (Figure 2, Table 1). This confirms the method's suitability for further drug estimation studies.

Table 2: Absorbance of pravastatin sodium working solution at 239nm.

Conc.(µg/ml)	Absorbance
2	0.097±0.001
4	0.184±0.008
6	0.289±0.004
8	0.376±0.001
10	0.465±0.005
12	0.576±0.003
14	0.648±0.006
16	0.742±0.012
18	0.824±0.005
20	0.925±0.009

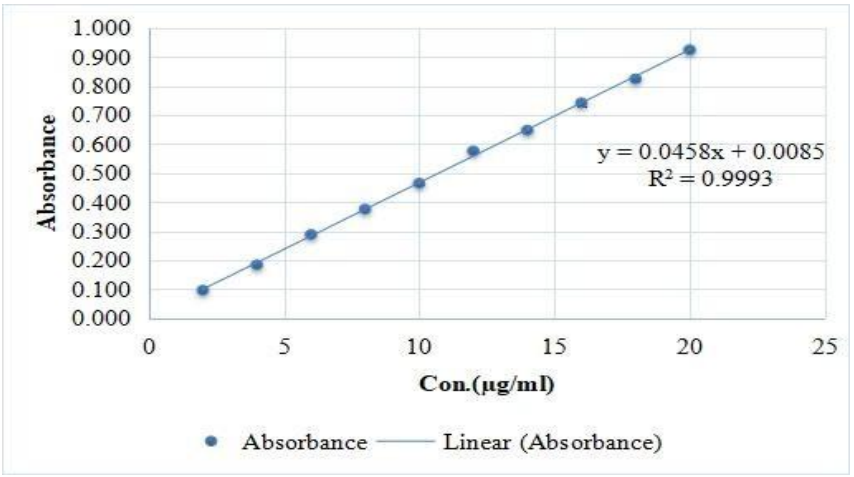

Figure 2: Calibration curve of pravastatin sodium in methanol at 239 nm

- **Solubility Study:**

The solubility profile of pravastatin sodium (Table 2, Figure 3) showed that the drug is freely soluble in methanol (108.96 ± 0.93 mg/ml) and water (102.18 ± 0.96 mg/ml), indicating its hydrophilic nature.

Table 2: Solubility of pravastatin sodium in various solvents

Solvent	Amount (mg/ml)	Outcome
Water	102.18±0.96	Freely soluble
Methanol	108.96±0.93	Freely soluble
Ethanol	74.74±0.68	Soluble
Chloroform	0.20±0.01	Very slightly soluble
Phosphate buffer pH 6.8	26.08±0.27	Soluble

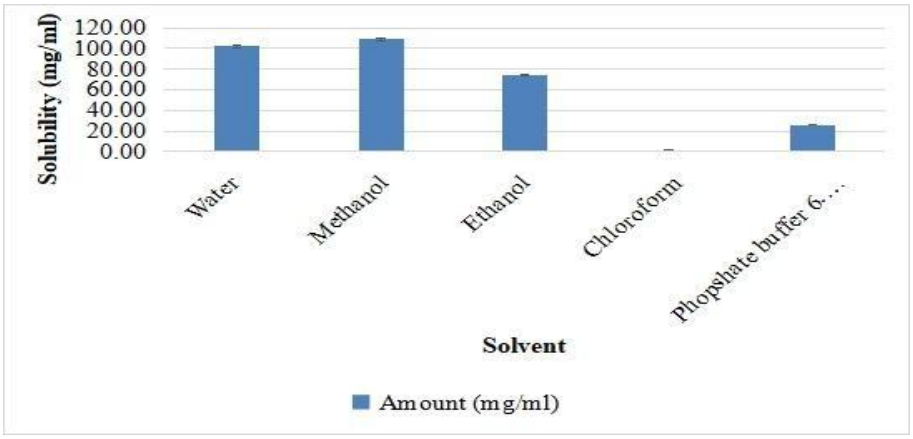

Figure 3: Solubility of pravastatin sodium in different solvents

- **Partition Coefficient**

The log P value of pravastatin sodium was -0.228 ± 0.019 in a water/n-octanol system, indicating its hydrophilic behavior, which aligns with reported literature. (148)

- **FTIR Spectroscopy**

FTIR analysis of the pure drug showed characteristic peaks: 3363 cm^{-1} (O-H), 2981 cm^{-1} and 2880 cm^{-1} (C-H stretching), 1724 cm^{-1} (C=O), 1560 cm^{-1} (C=C), and 1038 cm^{-1} (C-O), which confirmed the identity of pravastatin sodium (Figure 4). The FTIR spectrum of the selected formulation (G2DPN14) showed the same characteristic peaks but with reduced intensity, confirming successful encapsulation of the drug within the niosomal matrix (Figure 5).

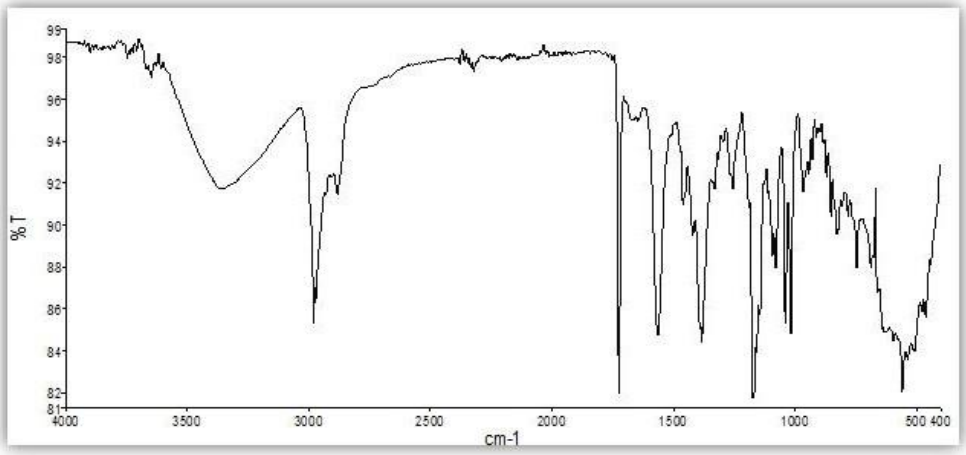

Figure 4: FTIR spectrum of pravastatin sodium (pure drug)

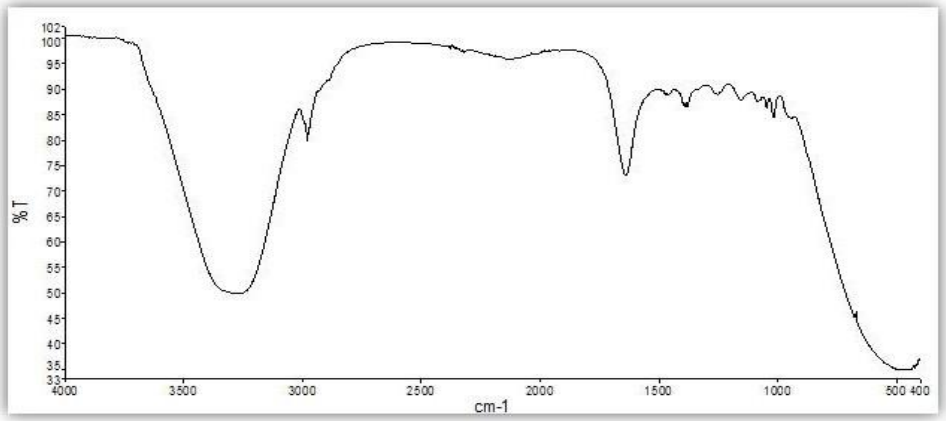

Figure 5: FTIR spectrum of niosomal gel formulation (G2DPN14)

3.2 Preparation and Optimization of Pravastatin Sodium-Loaded Niosomes

In the present investigation, pravastatin sodium-loaded niosomes were formulated using the reverse phase evaporation technique. This method has been widely reported for enhancing the encapsulation efficiency of hydrophilic drugs due to the formation of unilamellar or multilamellar vesicles with large internal aqueous cores. Span 60 (sorbitan monostearate), a non-ionic surfactant, was primarily used due to its saturated alkyl chain, higher phase transition temperature, and oxidative stability—offering advantages over unsaturated lipid-based systems such as liposomes

- **Effect of Surfactant Type on Niosomal Characteristics**

Four different surfactants—Span 60, Span 80, Tween 80, and Tween 60—were employed to investigate their influence on the physical appearance, pH, and entrapment efficiency of pravastatin sodium-loaded niosomes. As shown in Table 1, the formulation containing Span 60 (PN1) demonstrated the highest drug entrapment (73.80 ± 0.27%) and formed a uniform,

homogenous dispersion with an acceptable pH (5.26 ± 0.02). In contrast, Tween-based formulations (PN3 and PN4) exhibited drug precipitation and poor encapsulation, suggesting incompatibility between hydrophilic head groups of Tweens and the bilayer environment needed for effective drug entrapment. The observed differences in entrapment efficiency can be attributed to the surfactant's phase transition temperature (Tc), which impacts membrane rigidity. Span 60 possesses a higher Tc (~53°C) than Span 80 (-12°C), leading to more stable vesicles with reduced fluidity and leakage

Table 4: Effect of surfactant type on physical appearance, pH, and drug entrapment efficiency.

Formulation Code	Formulation Code	Physical Appearance	pH	Entrapment Efficiency (%)
PN1	Span 60	Uniform, homogenous dispersion	5.26 ± 0.02	73.80 ± 0.27
PN2	Span 80	Uniform, homogenous dispersion	5.14 ± 0.03	49.11 ± 0.85
PN3	Tween 80	Translucent with drug precipitation	5.11 ± 0.03	28.02 ± 0.81
PN4	Tween 60	Translucent with drug precipitation	5.35 ± 0.04	14.00 ± 0.49

- **Effect of Span 60 Molar Ratio**

To assess the effect of Span 60 concentration on niosome performance, formulations were prepared with molar ratios of 3, 5, 7, and 9. The results (Table 2) showed a significant increase in entrapment efficiency from 41.72 ± 0.32% (PN5, 3 molar) to 73.80 ± 0.27% (PN1, 7 molar). Increasing the Span 60 content likely enhanced bilayer formation by providing more lipid content for vesicle assembly and increasing the hydrophobic environment available for drug incorporation

However, further increase to 9 molar (PN7) slightly reduced entrapment efficiency (70.37 ± 0.19%), possibly due to vesicle destabilization and leakage from excessive surfactant levels, consistent with previous studies

Table 5: Effect of Span 60 molar ratio on niosomal characteristics.

Formulation Code	Molar Ratio (Span 60)	Physical Appearance	pH	Entrapment Efficiency (%)
PN5	3	Uniform, homogenous dispersion	5.14 ± 0.04	41.72 ± 0.32
PN6	5	Uniform, homogenous dispersion	5.32 ± 0.04	59.17 ± 0.37
PN1	7	Uniform, homogenous dispersion	5.26 ± 0.02	73.80 ± 0.27
PN7	9	Uniform, homogenous dispersion	5.29 ± 0.03	70.37 ± 0.19

- **Effect of Cholesterol Molar Ratio**

Cholesterol is a key component in niosomal formulations, influencing membrane stability, fluidity, and drug retention. In this study, molar ratios of 1, 2, 3, and 4 were evaluated (Table 3). Increasing cholesterol concentration from 1 molar (PN8) to 3 molar (PN1) improved drug entrapment from 32.73 ± 0.85% to 73.80 ± 0.27%. This can be attributed to the stabilizing effect of cholesterol on the bilayer, which prevents leaching of hydrophilic drugs and reduces membrane permeability. However, at 4 molars (PN10), a decline in entrapment efficiency (64.52 ± 0.56%) was observed, likely due to steric hindrance or competition for space within the bilayer, which reduces drug incorporation efficiency.

Table 6: Effect of cholesterol molar ratio on niosomal characteristics.

Formulation Code	Molar Ratio (Cholesterol)	Physical Appearance	pH	Entrapment Efficiency (%)
PN8	1	Non-uniform dispersion	5.04 ± 0.03	32.73 ± 0.85
PN9	2	Uniform, homogenous dispersion	5.16 ± 0.02	49.75 ± 0.64
PN1	3	Uniform, homogenous dispersion	5.26 ± 0.02	73.80 ± 0.27
PN10	4	Uniform, homogenous dispersion	5.31 ± 0.02	64.52 ± 0.56

3.3 Optimization of Pravastatin Sodium-Loaded Niosomes Using Central Composite Design

To optimize the formulation of pravastatin sodium-loaded niosomes, a central composite design (CCD) was employed to evaluate the effects of two independent variables: the molar concentrations of Span 60 (A) and cholesterol (B). The primary response analyzed was the percentage entrapment efficiency (EE%). The design included 13 experimental runs that systematically varied the two formulation parameters. Three-dimensional (3D) response surface plots were used to interpret the influence of these variables on EE%. The objective was to identify an optimized formulation with the highest possible entrapment efficiency. The range and levels of formulation variables used in the CCD are presented in Table 7.6, and the corresponding responses are listed in Table 7.7.

Table 7: Central composite design variables and response for pravastatin sodium-loaded niosomes.

Factor	Name	Units	Low Actual	High Actual	Low Coded	High Coded	Mean
A	Amount of Span 60	molar	5	9	-1.000	1.000	7
B	Amount of cholesterol	molar	2	4	-1.000	1.000	3
Y_1	Entrapment Efficiency	(%)	-	-	-	-	-

Table 8: Central composite design batches and their corresponding entrapment efficiency (%EE).

Formulation Code	Span 60 (molar)	Cholesterol (molar)	EE (%)
DPN1	7.00	3.000	73.826
DPN2	4.172	3.000	55.101

DPN3	5.00	4.000	61.523
DPN4	9.828	3.000	65.055
DPN5	9.00	2.000	58.098
DPN6	9.00	4.000	71.246
DPN7	7.00	1.586	54.994
DPN8	7.00	3.000	73.858
DPN9	5.00	2.000	53.603
DPN10	7.00	3.000	74.061
DPN11	7.00	4.414	69.443
DPN12	7.00	3.000	73.569
DPN13	7.00	3.000	73.387

- **Effect of Formulation Variables on Entrapment Efficiency**

Entrapment efficiency is a crucial parameter in the development of colloidal drug delivery systems. In this study, EE% ranged from 53.603 ± 0.642% to 74.061 ± 0.330% (Table 7.7). The influence of Span 60 and cholesterol concentrations on EE% was investigated to optimize drug encapsulation within niosomal vesicles.

- **ANOVA and Model Fitting**

The significance and adequacy of the quadratic model were assessed via analysis of variance (ANOVA), as shown in Table 7.8. The model exhibited a high degree of statistical significance ($p < 0.0001$), with an F-value of 3428.481. Individual contributions from Span 60 (Factor A) and cholesterol (Factor B), their interaction (AB), and their quadratic effects (A^2 and B^2) were all significant ($p < 0.0001$).

Table 9. ANOVA for quadratic model fitting of EE% response.

Source	Sum of Squares	F-value	p-value	Significance
Model	815.875	3428.481	< 0.0001	Significant
A - Span 60	100.080	2102.795	< 0.0001	
B - Cholesterol	215.310	4523.893	< 0.0001	
AB	6.834	143.591	< 0.0001	
A^2	325.357	6836.093	< 0.0001	
B^2	231.488	4863.802	< 0.0001	
Residual	0.333	-	-	
Lack of Fit	0.055	0.262	0.8497	Not significant
Pure Error	0.278	-	-	
Correlation Total	816.209	-	-	
R^2	0.999	-	-	
Adjusted R^2	0.999	-	-	
Predicted R^2	0.998	-	-	
Adequate Precision	135.112			

The regression model for entrapment efficiency (Y) is expressed by the following polynomial equation: {EE% (Y)} = 73.740 + 3.537A + 5.188B + 1.307AB - 6.839A^2 - 5.769B^2

Positive coefficients of A and B indicate a synergistic effect of Span 60 and cholesterol on drug entrapment, while negative quadratic terms suggest an optimal range beyond which further increases reduce efficiency.

- **Response Surface Analysis**

Contour and 3D surface plots (Figure 7.6A and 7.6B) were generated to visualize the interaction between formulation variables and EE%. It was evident that increasing both Span 60 and cholesterol concentrations positively influenced drug entrapment. These findings align with previous studies that emphasize the role of non-ionic surfactants and lipid stabilizers in enhancing vesicle integrity and drug loading efficiency. Similar outcomes were reported by Ghazwani et al., who demonstrated the beneficial effect of surfactant concentration on the encapsulation of carvacrol oil in niosomal formulations

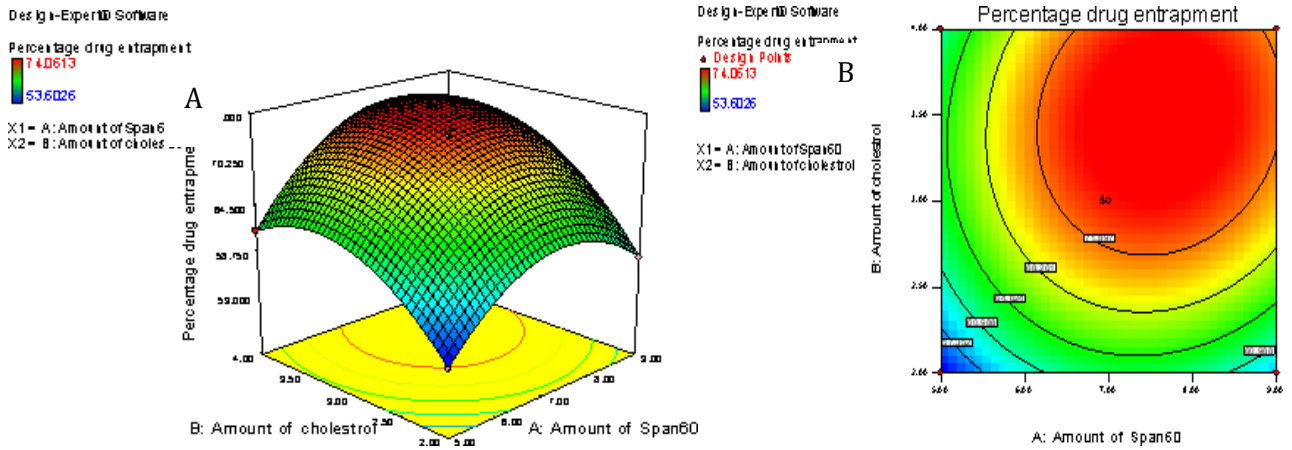

Figure 7.6. Response surface plots depicting the effect of Span 60 and cholesterol on entrapment efficiency: (A) Contour plot; (B) 3D surface plot.

- **Numerical Optimization**

Numerical optimization using Design-Expert® software was conducted to determine the ideal levels of formulation variables for maximum EE%. The optimized formulation comprised 7.55 molar Span 60 and 3.64 molar cholesterol, with a desirability score of 1.0. The predicted EE% was 75.377%, while the experimentally obtained EE% was 74.661 ± 0.260%, demonstrating strong agreement between predicted and actual values, thus confirming the model's validity.

3.4 n-vitro Characterization of Pravastatin Sodium-Loaded Niosomes

- **Physical Appearance**

The physical characteristics of all pravastatin sodium-loaded niosomal formulations (DPN1–DPN13) were assessed through visual observation. As summarized in **Table 10.** all formulations exhibited uniform and homogeneous dispersion without any signs of aggregation or phase separation, indicating successful noisome formation and physical stability.

Table 10: Physical appearance of pravastatin sodium-loaded niosomal formulations

Formulation Code	Physical Appearance
DPN1–DPN13	Uniform and homogeneous dispersion

- **pH Evaluation**

The pH of niosomal formulations was measured to ensure compatibility with topical and transdermal application, as well as to assess formulation stability. As presented in **Table 11:** the pH values ranged from **5.243 ± 0.042 to 5.780 ± 0.010**, falling within the physiologically acceptable range and indicating suitability for dermal application without irritation.

Table 11: pH values of pravastatin sodium-loaded niosomal formulations

Formulation Code	pH (Mean ± SD)
DPN1	5.563 ± 0.250
DPN2	5.647 ± 0.045
DPN3	5.300 ± 0.260
DPN4	5.513 ± 0.035
DPN5	5.780 ± 0.010
DPN6	5.620 ± 0.036
DPN7	5.343 ± 0.050
DPN8	5.413 ± 0.015
DPN9	5.753 ± 0.045
DPN10	5.543 ± 0.040
DPN11	5.243 ± 0.042
DPN12	5.350 ± 0.044
DPN13	5.540 ± 0.062

- **Percentage of Drug Entrapment**

Entrapment efficiency (EE%) is a critical parameter for evaluating the loading capacity and effectiveness of niosomal carriers. The EE% for pravastatin sodium-loaded Niosomes varied among the formulations, with values ranging from **53.603 ± 0.642% (DPN9)** to **74.061 ± 0.330% (DPN10)**, as detailed in **Table 12.** and illustrated in **Figure 7**. The variation in EE% can be attributed to the differing concentrations of Span 60 and cholesterol, which influence the bilayer stability and drug solubilization within the vesicles.

Table 12: Entrapment efficiency of pravastatin sodium-loaded niosomal formulations

Formulation Code	Entrapment Efficiency (% ± SD)
DPN1	73.826 ± 0.177
DPN2	55.101 ± 0.490
DPN3	61.523 ± 0.668
DPN4	65.055 ± 0.742
DPN5	58.098 ± 0.321
DPN6	71.246 ± 0.201
DPN7	54.994 ± 0.808
DPN8	73.858 ± 0.219
DPN9	53.603 ± 0.642
DPN10	74.061 ± 0.330
DPN11	69.443 ± 0.668
DPN12	73.569 ± 0.245
DPN13	73.387 ± 0.267

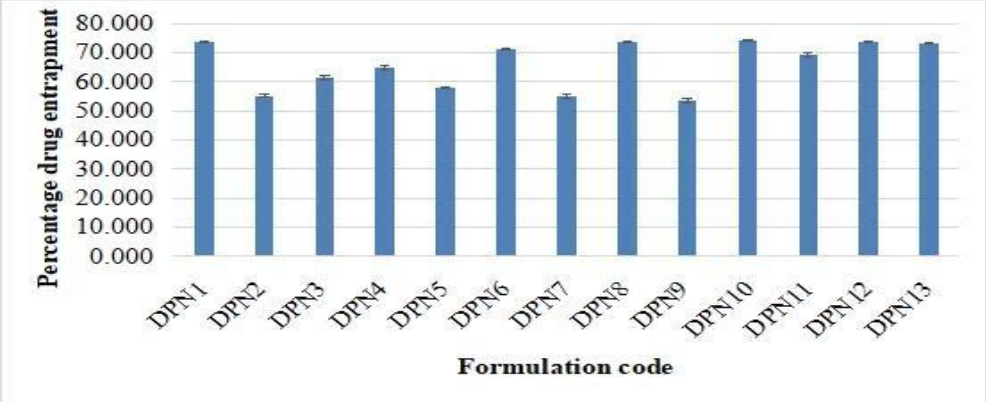

Figure 7. Percentage of drug entrapment of pravastatin sodium-loaded niosomal formulations

3.5 In-vitro Characterization of Optimized Niosomal Formulation (DPN14)

The optimized formulation, DPN14, was selected based on its high drug entrapment efficiency and desirable physicochemical characteristics. The in-vitro evaluation parameters including physical appearance, pH, and drug entrapment efficiency are summarized in **Table 13**.

Table 13. In-vitro characterization of optimized pravastatin sodium-loaded niosomal formulation (DPN14)

S. No.	Formulation Code	Physical Appearance	pH (Mean ± SD)	Entrapment Efficiency (% ± SD)
1.	DPN14	Uniform and homogeneous dispersion	5.25 ± 0.095	74.661 ± 0.260

- **Vesicle Size, Polydispersity Index (PDI), and Zeta Potential**

The vesicle size, polydispersity index (PDI), and zeta potential of formulation DPN14 were evaluated using dynamic light scattering (DLS). As depicted in **Figure 8**, the vesicle size was found to be **342.6 nm**, with a PDI of **0.166**, indicating a narrow size distribution and uniformity in the vesicle population. The zeta potential, shown in **Figure 9**, was recorded as **–28.2 mV**, suggesting good electrostatic stability of the niosomal suspension due to sufficient repulsion between vesicles.

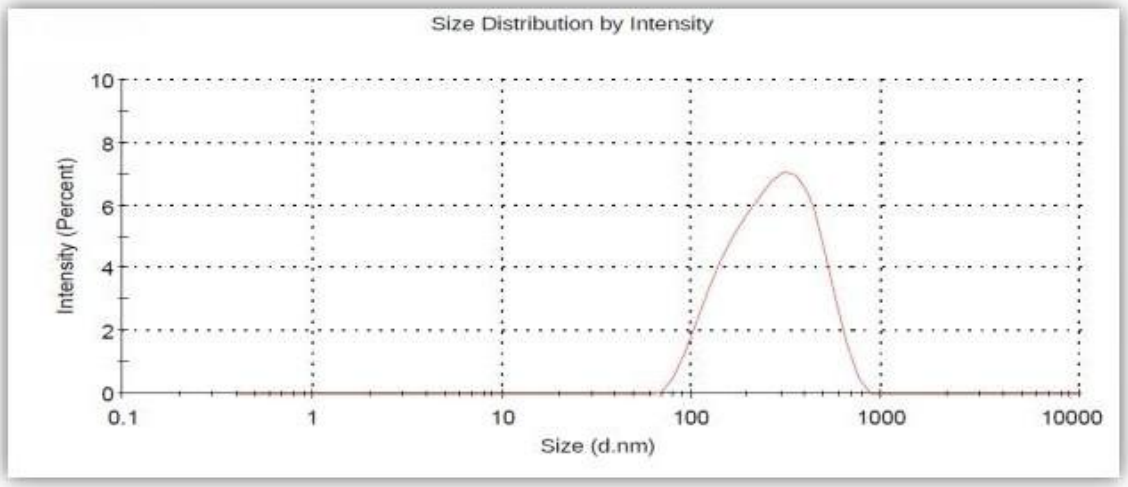

Figure 8: Vesicle size distribution of optimized formulation DPN14

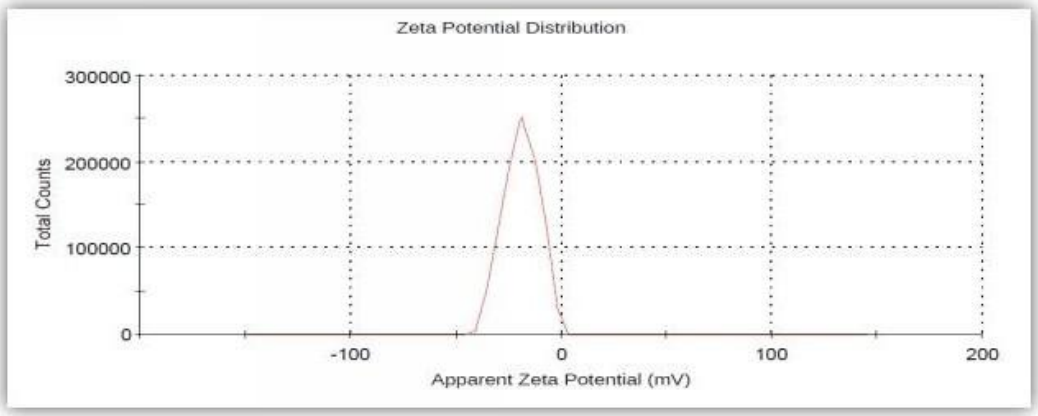

Figure 9: Zeta potential of optimized formulation DPN14

- **Transmission electron microscopy**

- Morphological analysis of the optimized formulation DPN14 was performed using transmission electron microscopy. As shown in **Figure 10**, the Niosomes appeared as discrete, spherical vesicles with a well-defined bilayer structure, confirming the successful formation of vesicular systems. The morphology corroborated the results of vesicle size analysis and demonstrated uniformity in structure.

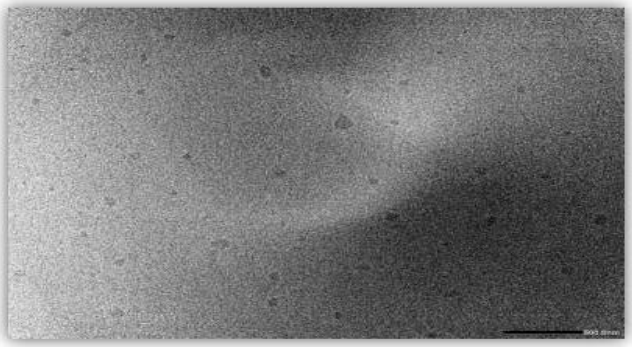

Figure 10. Transmission electron microscopy (TEM) image of formulation DPN14

3.6 In-vitro Characterization of Pravastatin Sodium-Loaded Niosomal Gel

- **Physical Appearance**

The physical appearance of pravastatin sodium-loaded niosomal gel formulations is presented in Table 14. All formulations were found to be homogenous, translucent, and uniform gels free from grittiness, indicating good formulation quality and proper dispersion of niosomes. However, formulation G1DPN14 exhibited comparatively lower viscosity than others.

Table 14: Physical appearance of pravastatin sodium-loaded niosomal gel formulations

S. No.	Formulation Code	Physical Appearance
1.	G1DPN14	Translucent, uniform gel, less viscous
2.	G2DPN14	Homogeneous, translucent, uniform gel, free from grittiness
3.	G3DPN14	Homogeneous, translucent, uniform gel, free from grittiness
4	G4DPN14	Homogeneous, translucent, uniform gel, free from grittiness

3.6.2. pH Evaluation

Table 7.14 summarizes the pH values of the gel formulations, which ranged from 5.183 ± 0.035 to 5.507 ± 0.038. These values are close to the physiological pH of the skin, indicating that the formulations are unlikely to cause irritation upon transdermal application.

Table 15: pH of pravastatin sodium-loaded niosomal gel formulations

S. No.	Formulation Code	pH
1.	G1DPN14	5.183 ± 0.035
2.	G2DPN14	5.347 ± 0.042
3.	G3DPN14	5.380 ± 0.030
4.	G4DPN14	5.507 ± 0.038

3.6.3. Spreadability

Spreadability is a critical parameter influencing gel application and patient compliance. As shown in Table 16, spreadability ranged from 4.929 ± 0.194 to 28.725 ± 1.422 g·cm/s. A negative correlation was observed between the spreadability and carbopol concentration, as increased polymer concentration leads to higher crosslinking and reduced spreadability.

Table 16: Spreadability of pravastatin sodium-loaded niosomal gel formulations

S. No.	Formulation Code	Spreadability (g·cm/s)
1.	G1DPN14	28.725 ± 1.422
2.	G2DPN14	14.597 ± 0.979
3.	G3DPN14	8.724 ± 0.499
4.	G4DPN14	4.929 ± 0.194

3.6.4. Viscosity

Viscosity is a key determinant of gel consistency and application ease. As shown in Table 17, the viscosity increased with higher carbopol content, ranging from 1883.33 ± 2.08 to 5115.67 ± 3.05 cP. This indicates a direct correlation between carbopol concentration and gel viscosity, with 1% w/w yielding optimal viscosity for transdermal application.

Table 17: Viscosity of pravastatin sodium-loaded niosomal gel formulations

S. No.	Formulation Code	Viscosity (cP)
1.	G1DPN14	1883.33 ± 2.08
2.	G2DPN14	2993.67 ± 2.52
3.	G3DPN14	3774.33 ± 3.51
4.	G4DPN14	5115.67 ± 3.06

3.6.5. Drug Content

The percentage drug content of the formulations is reported in Table 18. Drug content ranged from 93.92 ± 0.96% to 99.27 ± 0.49%. Formulations G2DPN14 and G3DPN14 exhibited the highest drug content, suggesting efficient drug entrapment and uniform distribution within the niosomal gel system.

Table 18: Drug content of pravastatin sodium-loaded niosomal gel formulations

S. No.	Formulation Code	Drug Content (%)
1.	G1DPN14	95.52 ± 0.85
2.	G2DPN14	98.84 ± 0.93
3.	G3DPN14	99.27 ± 0.49
4	G4DPN14	93.92 ± 0.96

3.6.6. In-vitro Drug Release

The cumulative percentage drug release profiles for formulations G2DPN14, G3DPN14, and control gel are presented in Table 19. After 24 hours, the cumulative release was significantly higher for G2DPN14 (96.96 ± 0.96%) and G3DPN14 (81.17 ± 0.60%) compared to the control gel (30.16 ± 0.91%). These findings confirm that niosomal formulations enhance drug release, likely due to the vesicular structure and surfactant-assisted penetration across the skin barrier.

Table 19: Cumulative drug release (%) of selected formulations

Time (h)	Control Gel	G2DPN14	G3DPN14
0	0.00 ± 0.00	0.00 ± 0.00	0.00 ± 0.00
0.25	8.81 ± 0.14	8.28 ± 0.61	6.17 ± 0.34
0.5	12.19 ± 0.41	12.61 ± 0.09	10.18 ± 0.42
1	14.36 ± 0.76	21.12 ± 0.21	18.44 ± 0.22
2	16.22 ± 0.43	32.91 ± 0.28	23.63 ± 0.08
4	21.91 ± 0.22	49.82 ± 0.35	37.23 ± 0.28
8	26.77 ± 0.14	65.15 ± 0.15	49.33 ± 0.69
10	28.71 ± 0.35	83.13 ± 0.07	69.27 ± 0.16
12	30.16 ± 0.69	96.96 ± 0.96	79.37 ± 0.54
24	30.16 ± 0.91	95.62 ± 0.45	81.17 ± 0.60

3.6.7. Drug Release Kinetics

The release kinetics of G2DPN14 were analyzed using various models (Table 20). The best fit was observed with the Higuchi model (R^2 = 0.940), indicating a diffusion-controlled release mechanism. This suggests that the niosomal gel system functions as a reservoir for sustained drug delivery.

Table 20: Drug release kinetic model fitting for G2DPN14

Model	Regression Coefficient (R^2)
Zero Order	0.774
First Order	0.803
Higuchi Model	0.940
Korsmeyer-Peppas	0.579

4. CONCLUSION

The present study successfully developed and characterized pravastatin sodium-loaded niosomal gel formulations aimed at enhancing transdermal delivery. Among the four formulations, G2DPN14 and G3DPN14 exhibited optimal physicochemical properties, including homogeneity, translucency, suitable pH (close to skin pH), good spreadability, and acceptable viscosity for dermal application. The drug content in these formulations was found to be high, indicating uniform distribution of pravastatin sodium within the niosomal gel matrix. The in-vitro drug release studies revealed a significantly enhanced and sustained release profile for niosomal formulations compared to the control gel. The highest cumulative drug release was observed in the G2DPN14 formulation (96.95% over 24 hours), followed by G3DPN14 (81.17%), indicating the efficiency of the niosomal carrier system in promoting sustained drug release. Kinetic modeling of the release data further confirmed that the drug release from the G2DPN14 formulation followed Higuchi's model, suggesting a diffusion-controlled release mechanism. This supports the potential of niosomes as reservoir-type systems capable of maintaining prolonged therapeutic levels of pravastatin sodium. In conclusion, the developed pravastatin sodium-loaded niosomal gel represents a promising transdermal delivery system with improved drug permeation, sustained release, and skin compatibility. These findings pave the way for future in-vivo evaluations and clinical investigations to confirm its therapeutic potential and patient compliance in the management of hyperlipidemia and related disorders.

REFERENCES

[1] Furumoto, K., S. Nagayama, K. Ogawara, Y. Takakura, M. Hashida, K. Higaki, and T. Kimura. 2004. 'Hepatic uptake of negatively charged particles in rats: possible involvement of serum proteins in recognition by scavenger receptor', *J Control Release*, 97: 133-41.

[2] Hatanaka, T. 2000. 'Clinical pharmacokinetics of pravastatin: mechanisms of pharmacokinetic events', *Clin Pharmacokinet*, 39: 397-412.

[3] Manosroi, A., R. Chutoprapat, M. Abe, W. Manosroi, and J. Manosroi. 2012. 'Anti-aging efficacy of topical formulations containing niosomes entrapped with rice bran bioactive compounds', *Pharm Biol*, 50: 208-24.

[4] Marais, Suzanne. 2019. 'The use of apricot oil emulsions for the transdermal delivery of selected statins', North-West University (South-Africa). Potchefstroom Campus.

[5] Neuvonen, P. J., M. Niemi, and J. T. Backman. 2006. 'Drug interactions with lipid-lowering drugs: mechanisms and clinical relevance', *Clin Pharmacol Ther*, 80: 565-81.

[6] Prausnitz, M. R., and R. Langer. 2008. 'Transdermal drug delivery', *Nat Biotechnol*, 26: 1261-8.

[7] Reinoso, Raquel F, Brian A Telfer, and Malcolm Rowland. 1997. 'Tissue water content in rats measured by desiccation', *Journal of pharmacological and toxicological methods*, 38: 87-92.